Electronic Supplementary Material (ESI) for Journal of Materials Chemistry C.

Supporting Information

Birhodanines and their sulfur analogues for air-stable n-channel organic transistors

Kodai Iijima,[a] Yann Le Gal,[b] Toshiki Higashino,[ac] Dominique Lorcy,[b] and Takehiko Mori[a]*

Synthesis

All commercial chemicals and solvents were used without further purification. Methylamine (*ca*. 40% in water, M0137), ethylamine (*ca*. 33% in water, E0055), propylamine (P0520), butylamine (B0707) and dimethyl acetylene dicarboxylate (A0090) were obtained from TCI. Carbon disulfide (038-01246) was obtained from Wako. The data of Nuclear Magnetic Resonance spectrum (NMR) and Mass spectrum (MS) were obtained with a JEOL JNM-AL300 spectrometer and a JEOL JMS-Q1050GC mass spectrometer, respectively.

Titanocene complex (2-Me).

Under nitrogen atmosphere, to a −10 °C cooled solution of *N*-alkyl-1,3-thiazole-2-thione **1-*R*** (7.6 mmol)[8] in dry THF (50 ml) was added a solution of lithium diisopropylamide (LDA) freshly prepared from *n*-butyl lithium (*n*-BuLi) (11.5 mmol, 7.2 mL) and diisopropylamine (11.5 mmol, 1.6 mL) in 30 mL of dry THF. After stirring for 30 min at −10 °C, S_8 (11.5 mmol, 366 mg) was added and the solution was stirred for additional 30 min. To the medium a solution of LDA freshly prepared from n-BuLi (15.3 mmol, 9.6 mL) and diisopropylamine (15.3 mmol, 2.2 mL) in 30 mL of dry THF was added. The reaction mixture was stirred at −10 °C for 3 h and sulfur S_8

(12.6 mmol, 403 mg) was added. After 30 min, titanocene dichloride (9.92 mmol, 2.47 g) was added and stirred for 30 min at −10 °C and further stirred for 1 h at room temperature. The solution was evaporated *in vacuo* and extracted with dichloromethane and washed with water. The organic layer was dried over $MgSO_4$ and evaporated *in vacuo*. The crude product was purified by column chromatography using petroleum ether/dichloromethane (4/1) as eluent to afford **2-*R*** as a dark blue solid.

2-Me: Yield 56% (1.59 g), m.p.> 260 ºC. ^{1}H NMR (300 MHz, $CDCl_3$) δ 3.77 (s, 3H, CH_3), 5.51 (s, 5H, Cp), 6.13 (s, 5H, Cp); ^{13}C NMR (75 MHz, $CDCl_3$) δ 36.14 (CH_3), 107.9 (Cp), 112.3 (Cp), 131.2 (C=C), 144.6 (C=C), 190.4 (C=S); HRMS (ESI) calcd for $C_{14}H_{14}NS_4{}^{48}Ti$ $[M + H]^+$: 371.9489. Found: 371.9490.

2-Pr: Yield 48%, (1.45g). m.p. 192 ºC. ^{1}H NMR (300 MHz, $CDCl_3$) δ 1.03 (t, 3H, CH_3, J = 7.2 Hz), 1.85 (m, 2H, CH_2), 4.30 (m, 2H, CH_2), 5.51 (s, 5H, Cp), 6.12 (s, 5H, Cp); ^{13}C NMR (75 MHz, $CDCl_3$) δ 11.2 (CH_3), 20.8 (CH_2), 50.4 (CH_2), 107.8 (Cp), 112.2 (Cp), 131.5 (C=C), 144.5 (C=C), 190.2 (C=S); HRMS (ESI) calcd for $C_{16}H_{17}NNaS_4{}^{48}Ti$ $[M + Na]^+$: 421.96210. Found: 421.9623;

3-*R*.

To a solution of **2-*R*** (1.35 mmol) in 40 mL of dry THF was added triphosgene (2.7 mmol, 800 mg). The mixture was refluxed for 30 min. 10 mL of water was added and the solution was evaporated *in vacuo* and extracted with dichloromethane and washed with water. The organic layer was dried over $MgSO_4$ and evaporated *in vacuo*. The crude product was purified by column chromatography using petroleum ether/dichloromethane (4/1) as eluent to afford **3-*R*** as a brown solid.

3-Me: Yield: 70% (210 mg). m.p.: 158ºC. ^{1}H NMR (300 MHz, $CDCl_3$) δ 3.71 (s); ^{13}C

NMR (75 MHz, $CDCl_3$) δ 38.2 (CH_3), 102.6 (C=C), 127.1 (C=C), 186.6 (C=O), 187.7 (C=S); IR $\nu_{(C=S)}$ = 1349 cm^{-1}, $\nu_{(C=O)}$ =1650 cm^{-1}; HRMS (ESI) calcd for $C_5H_4NOS_4$ [M + H]$^+$: 221.91758. Found: 221.9177 ; Anal. calcd for $C_5H_3NOS_4$: C, 27.13; H, 1.37; N, 6.33. Found: C, 26.99; H, 1.29; N, 6.08.

3-Pr: Yield 76% (255 mg). ^{1}H NMR (300 MHz, $CDCl_3$) δ 1.02 (t, 3H, CH_3, J = 7.2 Hz), 1.87 (m, 2H, CH_2), 4.12 (m, 2H, CH_2); ^{13}C NMR (75 MHz, $CDCl_3$) δ 11.2 (CH_3), 20.8 (CH_2), 53.0 (CH_2), 103.0 (C=C), 126.6 (C=C), 187.0 (C=O), 187.2 (C=S); IR $\nu_{(C=S)}$ = 1379 cm^{-1}, $\nu_{(C=O)}$ =1652 cm^{-1}; HRMS (ASAP) calcd for $C_7H_7NOS_4$ [M + H]$^+$: 249.9888. Found: 249.9490; Anal. calcd for $C_{16}H_{17}NS_4Ti$: C, 33.71; H, 2.83; N, 5.62. Found: C, 33.91 ; H, 2.65 ; N, 5.64.

3,3'-Dimethyl-5,5'-bithiazolidinylidene-2,4,2',4'-tetrathione (SS-*R*). A solution of **3-*R*** (0.68 mmol) in 50 mL of toluene was refluxed overnight. 90% of the solution was evaporated in vacuo and the precipitate was filtered and washed with ethanol and dried in vacuo to afford **SS-*R*** as a purple solid. The product was purified by chromatography on silica gel using CH_2Cl_2 as eluent to afford **SS-*R*** as a dark purple powder. Crystals of sufficient quality for X-ray diffraction were obtained by slow evaporation of CH_2Cl_2.

SS-Me: Yield: 64% (70 mg). m.p. >260 ºC. ^{1}H NMR (300 MHz, , $(CD_3)_2SO$) δ 3.73 (s); ^{13}C NMR (75MHz) δ ; not enough soluble even in DMSO. HRMS (ASAP) calcd for $C_8H_6N_2S_6$ [M + H]$^+$: 322.89335. Found: 322.8932; Anal. calcd for $C_8H_6N_2S_6$ + 0.5 CH_2Cl_2: C, 27.97; H, 1.96; N, 7.68. Found: C, 27.25 ; H, 1.60 ; N, 7.67. UV-Vis: λ_{max}(nm) (ε[L.mol^{-1}.cm^{-1}] 560 (3632), 525 (3991), 350 (20756), 245 (12141).

SS-Pr: Yield 79% (101mg). m.p. >190 ºC. ^{1}H NMR (300MHz, $CDCl_3$) δ 0.98 (t, 3H,

CH_3, J = 7.4 Hz), 1.74 (m, 2H, CH_2), 4.46 (m, 2H, CH_2); ^{13}C NMR (75 MHz, $CDCl_3$) δ 11.3 (CH_3), 19.8 (CH_2), 49.6 (CH_2), 133.7 (C=C), 189.0 (C=S), 201.6 (C=S); HRMS (ESI) calcd for $C_{12}H_{14}N_2S_6$ $[M + H]^+$: 378.95595. Found: 378.9562; UV-Vis: λ_{max}(nm) (ε[$L.mol^{-1}.cm^{-1}$] 500 (3675), 350 (25401), 245 (13840).

3,3'-Dialkyl-2,2'-dithioxo-[5,5']bithiazolidinylidene-4,4'-dione (OS-*R*)[12]

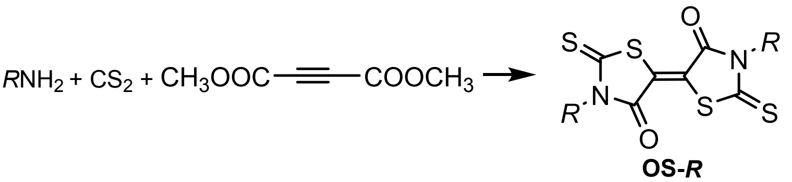

To a stirred solution of carbon disulfide (1.45 mL, 24 mmol) and dimethyl acetylene dicarboxylate (1.23 mL, 10 mmol) was added dropwise alkyl amine (20 mmol). When the vigorous and exothermic reaction ceased, ethanol (50 mL) was added. The resulting precipitate was collected by filtration, washed with ethanol and dried to give a yellow powder. The product was purified by recrystallization from toluene. For the fabrication of the thin-film transistors, the compound was further purified by sublimation under a vacuum of 10^{-4} Pa at 180°C for 24 h.

3,3'-Dimethyl-2,2'-dithioxo-[5,5']bithiazolidinylidene-4,4'-dione (OS-Me): Red needle, yield 0.36 g (12%), EIMS *m/z*: 290 [M^+]; ^1H NMR (300 MHz, $CDCl_3$) δ 3.42 (s, 6H, CH_3).

3,3'-Diethyl-2,2'-dithioxo-[5,5']bithiazolidinylidene-4,4'-dione (OS-Et): Orange plate, yield 0.78 g (24%), EIMS *m/z*: 318 [M^+]; ^1H NMR (300 MHz, $CDCl_3$) δ 1.29 (t, 6H, J = 7.1 Hz, CH_3), 4.20 (q, 4H, J = 7.2 Hz, N-CH_2).

3,3'-Dipropyl-2,2'-dithioxo-[5,5']bithiazolidinylidene-4,4'-dione (OS-Pr): Orange plate, yield 1.35 g (39%), EIMS *m/z*: 346 [M^+]; ^1H NMR (300 MHz, $CDCl_3$) δ 0.96 (t, 6H, *J* = 7.4 Hz, CH_3), 1.80–1.61 (m, 4H, $C\underline{H}_2$-CH_3), 4.12–3.88 (m, 4H, N-CH_2).

3,3'-dibutyl-2,2'-dithioxo-[5,5']bithiazolidinylidene-4,4'-dione (OS-Bu): Orange plate, yield 0.25 g (7%), EIMS *m/z*: 374 [M^+]; ^1H NMR (300 MHz, $CDCl_3$) δ 0.95 (t, 6H, *J* = 7.3 Hz, CH_3), 1.44–1.32 (m, 4H, $C\underline{H}_2$-CH3), 1.73–1.63 (m, 4H, CH_2-$C\underline{H}_2$-CH_2), 4.11 (q, 4H, *J* = 7.4 Hz, N-CH_2).

Alternative preparation of OS-*R*

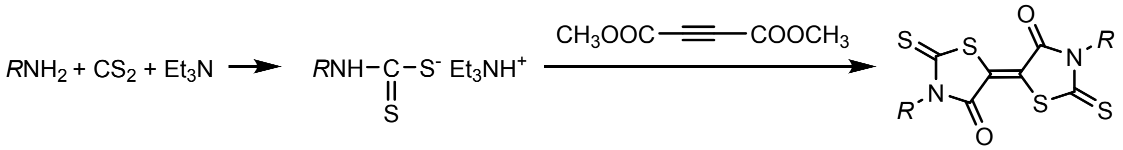

OS-*R*

Triethylammonium alkyl carbamate[13]

Alkylamine (20 mmol), carbon disulfide (1.83 g, 24 mmol), and triethylamine (6.09 g, 60 mmol) were reacted at room temperature. After 1 h, the formed precipitate was filtered to give a pale yellow solid in a nearly quantitative yield.

OS-*R*[14]

The carbamate (10 mmol) in 15 mL methanol was reacted with dimethyl acetylene dicarboxylate (0.71 g, 5 mmol) in 5 mL methanol. After 2 h, the formed precipitate was filtered to give an orange solid. The overall yields were very similar to the one-step reaction.

Cyclic Voltammetry (CV) and ultraviolet-visible spectroscopy (UV-Vis)

Reduction potentials were measured by cyclic voltammetry (CV) on an ALS model 701E electrochemical analyzer (Fig. 1(a)) using dry dichloromethane as a solvent and tetrabutylammonium hexafluorophosphate as an electrolyte. The working electrode was glassy carbon, and the counter electrode was platinum. Ag in a 0.1 M $AgNO_3$ solution was used as a reference electrode. The LUMO levels were estimated by assuming the reference energy level of ferrocene/ferrocenium (Fc/Fc^+: $E^{1/2} = +0.195$ V *vs*. $Ag/AgNO_3$ measured under the identical conditions) to be 4.8 eV from the vacuum level.[15]

UV-Vis spectra were collected on a shimadzu UV1800 Spectrophotometer in CH_2Cl_2.

Molecular orbitals

Molecular orbitals were calculated by Gaussian 09 package at B3LYP/6-311G(d,p) level.[17] The LUMOs and the anionic form were shown in Fig. S1.

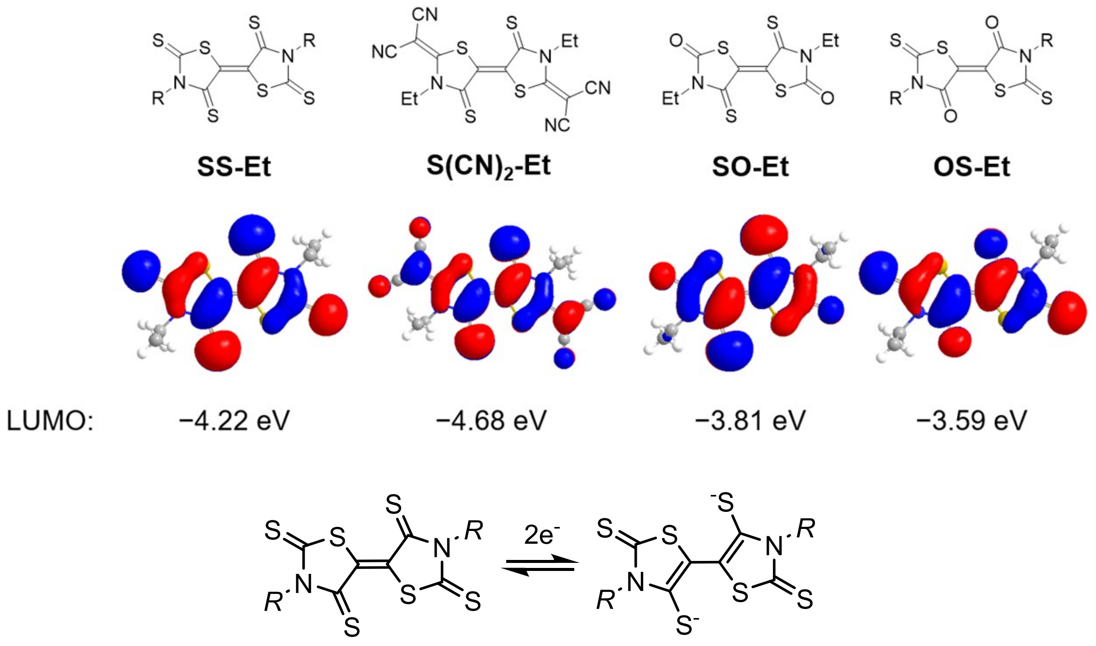

Figure S1. LUMOs of **SS-Et**, **S(CN)$_2$-Et**, **SO-Et**, and **OS-Et**, and the anionic form.

Device fabrication and thin-film properties

The transistors were prepared by using a commercially available heavily doped *n*-type Si wafer with 300 nm SiO_2 insulator ($\varepsilon = 3.9$ and the capacitance of 11.5 nF cm^{-2}) as a gate.[S1] A passivation layer of TTC was evaporated ($\varepsilon = 2.5$ and 20 nm thickness with the capacitance of 106 nF cm^{-2}),[18] and the resulting overall capacitance of the gate dielectric was 10.4 nF cm^{-2}. Then the birhodanine derivatives (50 nm) were vacuum evaporated at a rate of 1.0 Å s^{-1} under a pressure of 10^{-3} Pa. Gold source and drain electrodes were evaporated through a shadow mask (L/W = 100/1000 μm) at a pressure of 10^{-3} Pa to accomplish the bottom-gate top-contact transistors. Transistor characteristics were measured with a Keithley 4200 semiconductor parameter analyzer under vacuum and in air. The mobility values were evaluated from the transconductance in the saturated region. The average values were average for at least four devices. The transfer and output characteristics are shown in Figs. S2-S4.

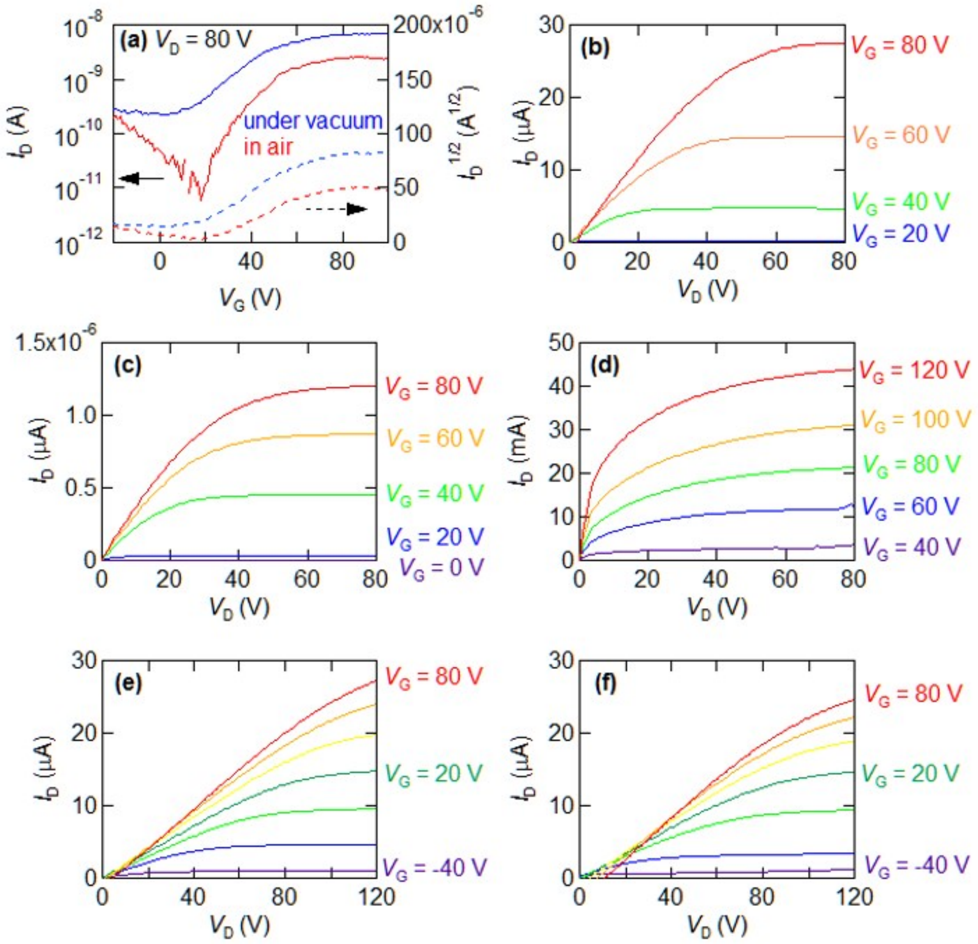

Figure S2. (a) Transfer characteristics of thin-film transistors based on **SS-Me**. (b) Output characteristics of a thin-film transistor based on **SS-Pr** measured under vacuum. Output characteristics of thin-film transistors based on **SS-Bu** measured (c) under vacuum, and (d) in air. Output characteristics of thin-film transistors based on **S(CN)$_2$-Et** measured (e) under vacuum, and (f) in air.

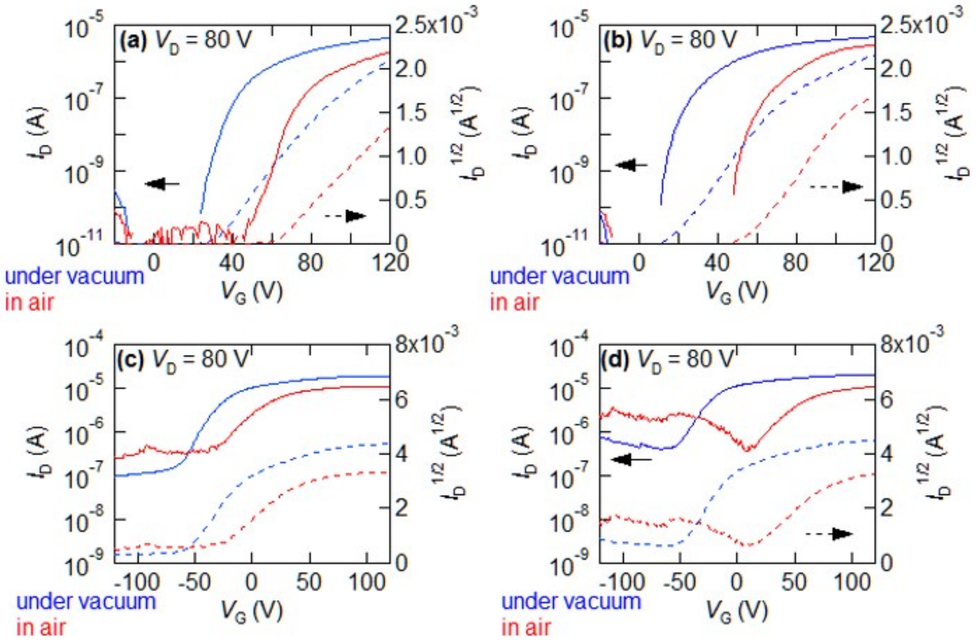

Figure S3. Transfer characteristics of thin-film transistors based on **SS-Bu** measured (a) after three-month storage under vacuum, and (b) after further three-month storage in air. Transfer characteristics of thin-film transistors based on **S(CN)$_2$-Et** measured (c) after three-month storage under vacuum, and (d) after further three-month storage in air.

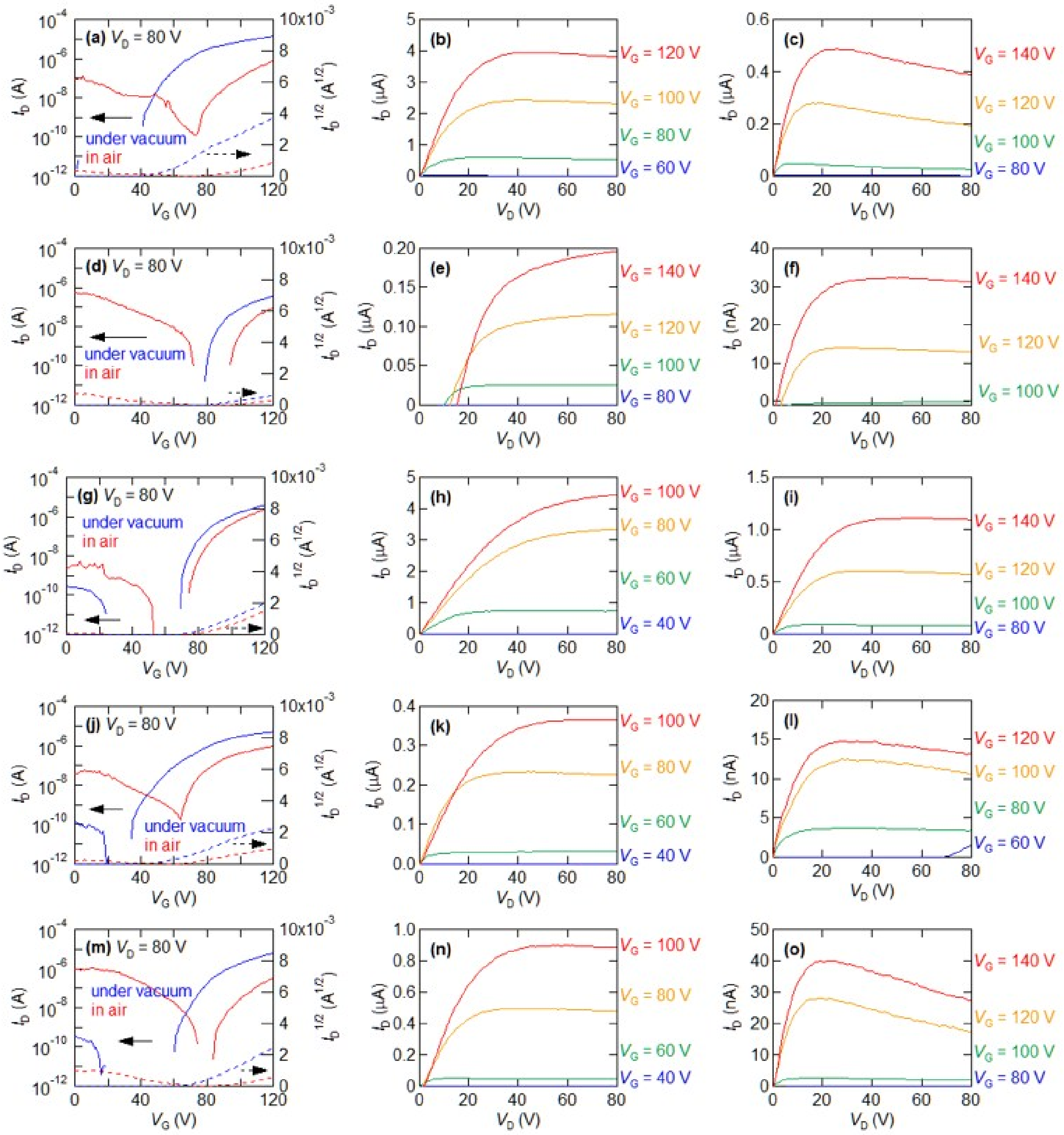

Figure S4. n-Channel characteristics of thin-film transistors based on **SO-Et** (a, b, and c) and **OS-*R*** (*R* = Me (d, e, and f), Et (g, h, and i), Pr (j, k, and l), and Bu (m, n, and o)). Transfer characteristics (a, d, g, j, and m) are measured together with output characteristics measured under vacuum (b, e, h, k, and n) and in air (c, f, i, l, and o).

Long-term stability of SS-Et transistors

In order to investigate the long-term stability of **SS-Et** thin-film transistors, the transfer characteristics are measured after storage under vacuum and in air (Fig. S5). The parameters are extracted as shown in Table S1.

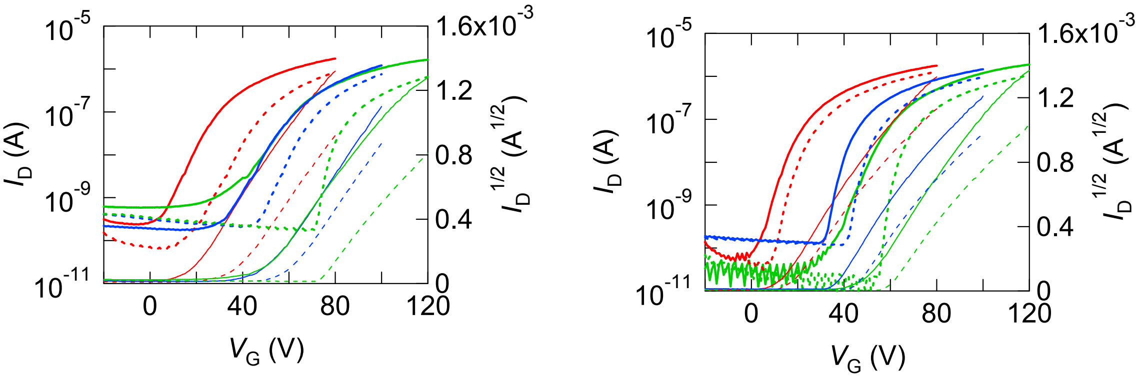

Figure S5. Transfer characteristics showing the long-term stability of **SS-Et** thin-film transistors with (a) Au and (b) (TTF)(TCNQ) source and drain electrodes.[S2] Measurement under vacuum (solid) and in air (dashed). After the measurements for the pristine devices (red), the measurements are repeated after ten weeks storage under vacuum (blue). Then the measurements are repeated after four weeks storage in air (green).

Table S1. Transistor characteristics of the **SS-Et** thin-film transistors extracted from Fig. S5.

Electrodes	Conditions	Measurements	μ_{ave} [μ max] ($\mathrm{cm^2\ V^{-1}\ s^{-1}}$)	V_T (V)	on/off
Au	pristine	under vacuum	5.9×10^{-3} [1.5×10^{-2}]	12	6×10^3
		in air	4.6×10^{-3} [1.2×10^{-2}]	31	4×10^3
	ten weeks under vacuum	under vacuum	6.5×10^{-3} [1.6×10^{-2}]	47	2×10^4
		in air	6.6×10^{-3} [1.4×10^{-2}]	59	2×10^3
	four weeks in air	under vacuum	8.1×10^{-3} [1.8×10^{-2}]	47	7×10^3
		in air	6.1×10^{-3} [1.7×10^{-2}]	69	2×10^4
(TTF)(TCNQ)	pristine	under vacuum	8.6×10^{-3} [1.4×10^{-2}]	12	4×10^4
		in air	6.7×10^{-3} [8.2×10^{-2}]	21	2×10^4
	ten weeks under vacuum	under vacuum	8.5×10^{-3} [1.4×10^{-2}]	38	6×10^4
		in air	7.5×10^{-3} [1.4×10^{-2}]	50	7×10^3
	four weeks in air	under vacuum	9.7×10^{-3} [1.8×10^{-2}]	63	6×10^4
		in air	6.9×10^{-3} [1.4×10^{-2}]	66	6×10^4

Crystal Structures

Crystals of **OS-Me**, **OS-Et**, **OS-Pr**, and **OS-Bu** for X-ray single crystal structure analyses were obtained by slow evaporation of toluene. The structure of **SO-Et** has been reported.[10] The diffraction data of **OS-Me**, **OS-Et**, and **OS-Bu** were collected by a Rigaku four-circle diffractometer (AFC-7R) with graphite-monochromatized Mo-$K\alpha$ radiation (λ = 0.71069 Å). The X-ray oscillation photographs of **OS-Pr** were taken using a RIGAKU R-AXIS RAPID II imaging plate with Cu-$K\alpha$ radiation from a rotation anode source with a confocal multilayer X-ray mirror (RIGAKU VM-Spider, λ = 1.54187 Å). The structures were solved by the direct method (SIR2008) and refined by the full matrix least-squares procedure (SHELXL).[S3,S4] Anisotropic thermal parameters were adopted for all non-hydrogen atoms. The crystal structures are depicted in Figs. S6-S11.

The transfer integrals, t_i, listed in **Table 1** were estimated from the molecular orbital calculations.[S5]

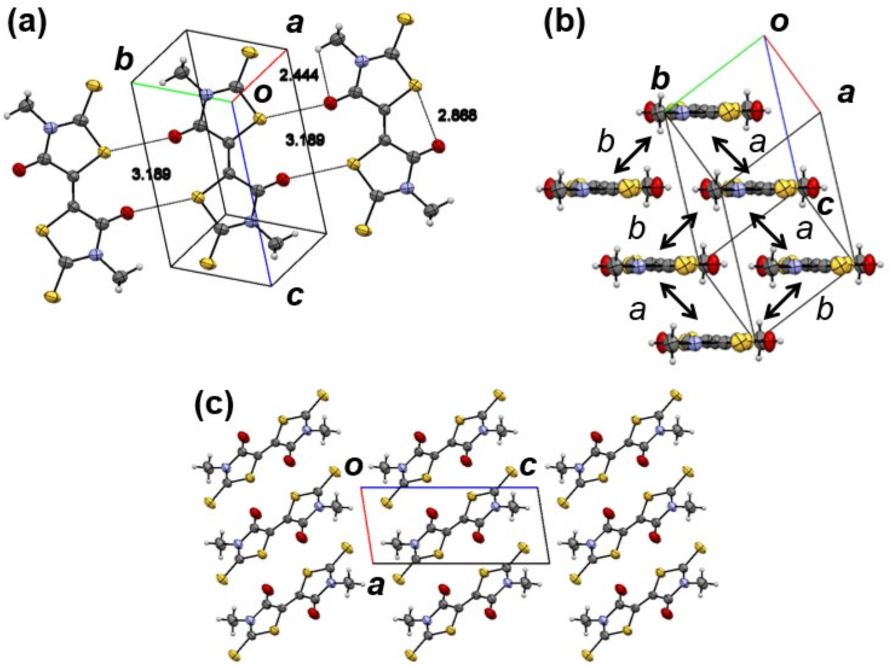

Figure S6. Crystal structure of **OS-Me** viewed along (a) the axis perpendicular to the molecular plane, (b) the molecular long axis, and (c) along the *b* axis. Short contacts shown in (a) are O–S (intra) = 2.868 Å, O–S (inter) = 3.189 Å, CH–O = 2.444 Å.

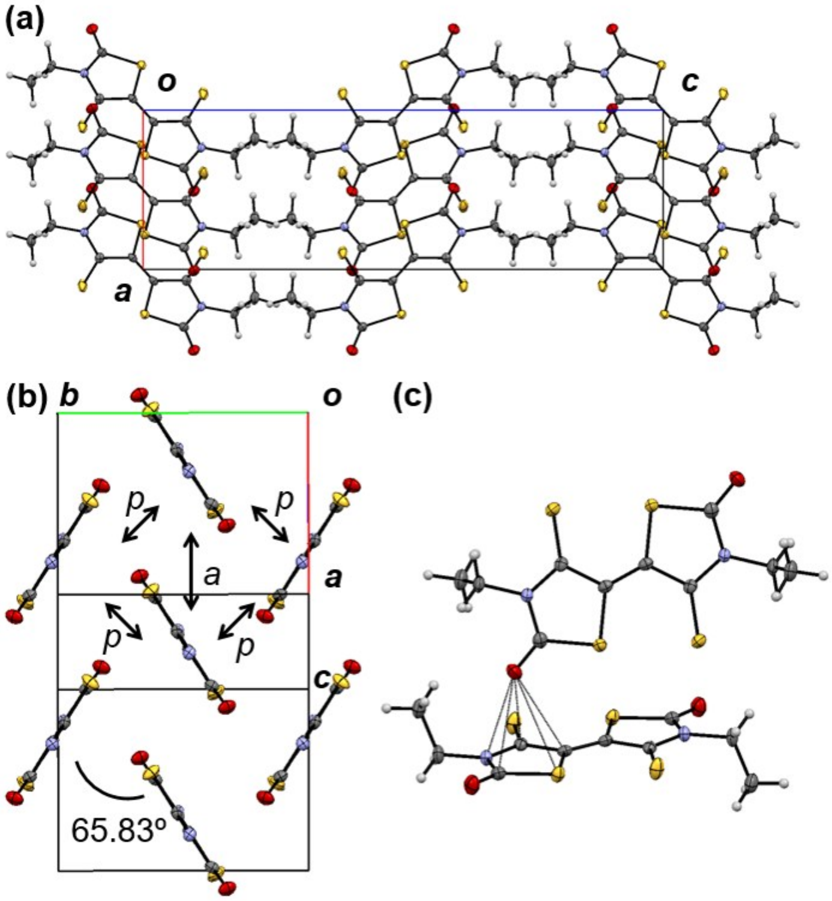

Figure S7. Crystal structure of **SO-Et**.[10] Crystal structure (a) viewed along the *b* axis, and (b) viewed along the molecular long axis (ethyl groups are omitted for clarity). Short contacts in (c) are O–N = 3.021 Å, O–C=O = 3.050 Å, O–C=S = 3.076 Å, O–C=C = 3.183 Å, O–S = 3.303 Å. (b) Crystal structure viewed along the molecular long axis (ethyl groups are omitted for clarity). Transfer integrals of the LUMO–LUMO interactions are $a = -27.0$ and $p = -3.2$ meV.

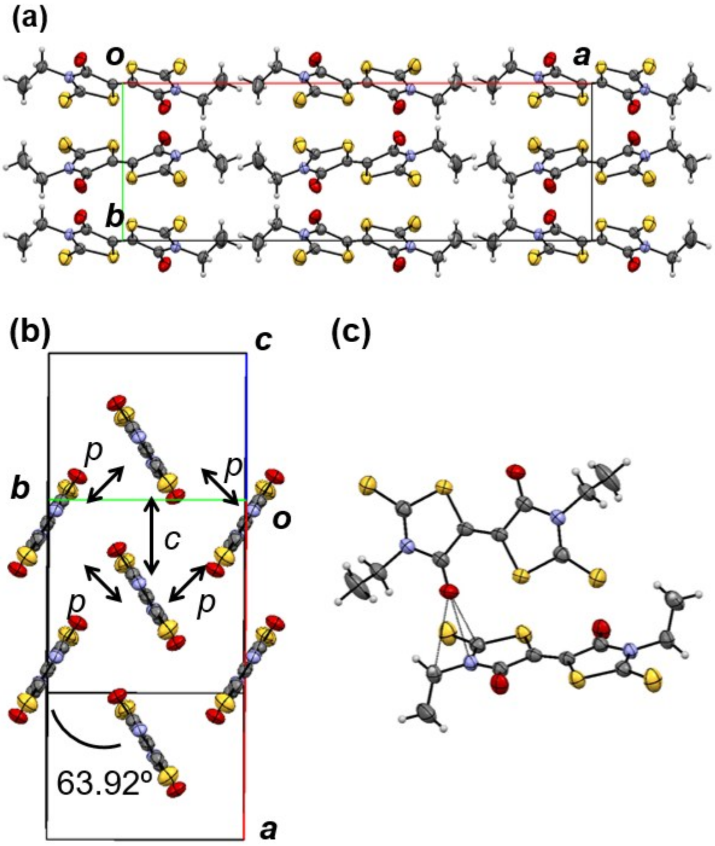

Figure S8. Crystal structure of **OS-Et** (a) viewed along the *c* axis, and (b) viewed along the molecular long axis (ethyl groups are omitted for clarity). Short contacts in (c) are O–N = 2.962 Å, O–C-N = 3.159 Å, O–C=S = 3.216 Å. Transfer integrals of the LUMO–LUMO interactions are $c = 2.5$ and $p = -16.1$ meV.

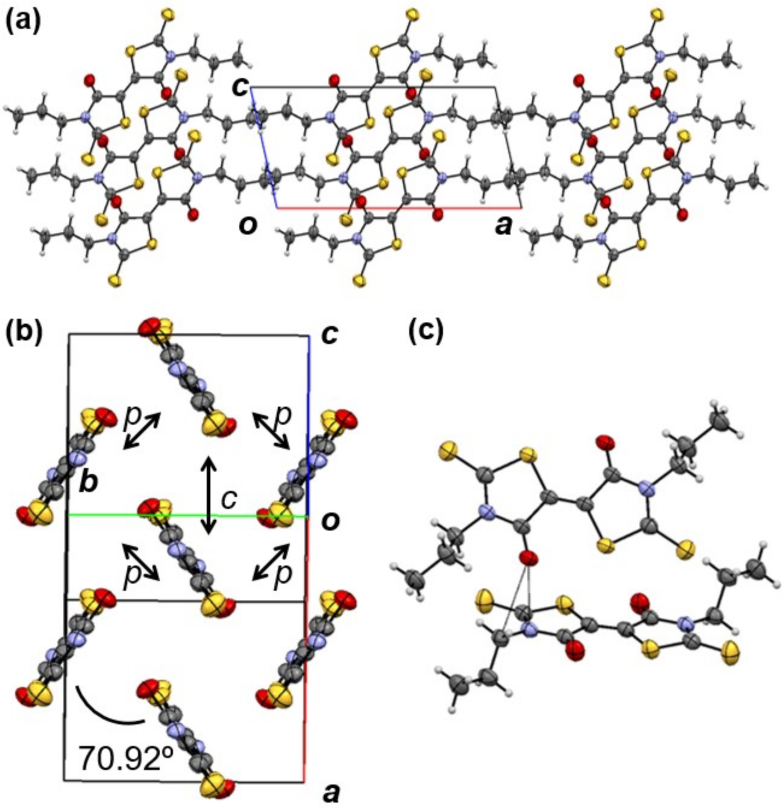

Figure S9. Crystal structure of **OS-Pr**. Crystal structure (a) viewed along the *b* axis, and (b) viewed along the molecular long axis (ethyl groups are omitted for clarity). Short contacts in (c) are O–N = 2.944 Å, O–C-N = 3.147. Transfer integrals of the LUMO–LUMO interactions are *c* = 2.0 and *p* = −9.0 meV.

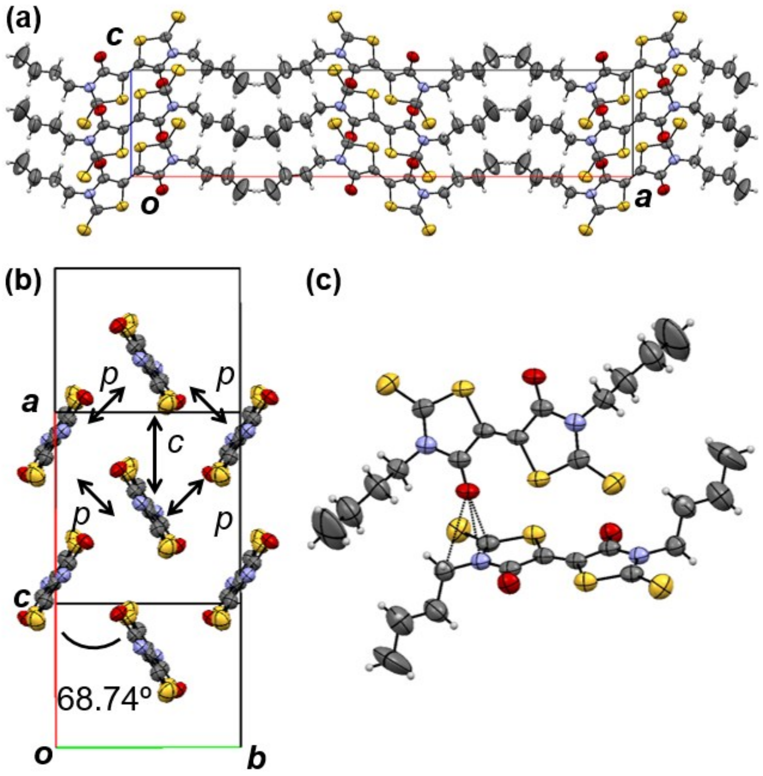

Figure S10. Crystal structure of **OS-Bu**. Crystal structure (a) viewed along the *b* axis, and (b) viewed along the molecular long axis (ethyl groups are omitted for clarity). Short contacts in (c) are O–N = 2.932 Å, O–C-N = 3.180 Å, O–C=S = 3.208 Å. Transfer integrals of the LUMO–LUMO interactions are *c* = 0.9 and *p* = −8.5 meV.

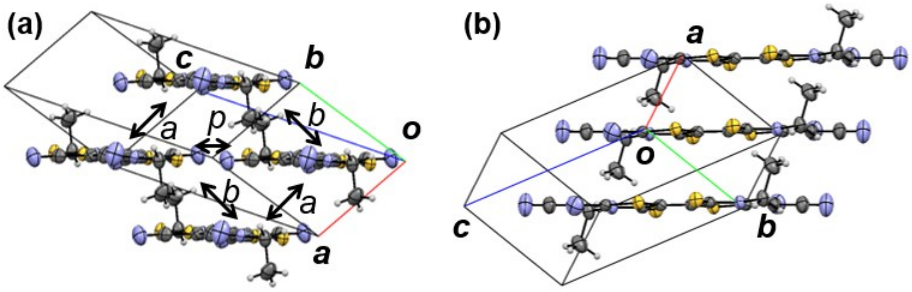

Figure S11. Crystal structure of **S(CN)$_2$-Et**.[11] Crystal structure (a) viewed along the molecular long axis, and (b) along the molecular short axis. Short S-S contacts are 3.692 Å and 3.886 Å. Transfer integrals of the LUMO–LUMO interactions are a = 56.9, b = −68.9 and p = −3.2 meV.

Thin film properties

X-ray diffraction analyses of thin films (50 nm) on TTC (20 nm) were performed by X'pert-Pro-MRD using the θ-2θ technique with Cu-$K\alpha$ radiation for $2° \leq 2\theta \leq 20°$. Since the observed d values (Fig. 6) agree with the lattice constants (Table 3), the tilt angles were estimated from the crystal structures as shown in Fig. S12. AFM images of thin films (50 nm) on TTC (20 nm) were taken by a SII scanning probe microscope system SPI3800N and SPA-300 by using a Si_3N_4 cantilever (Fig. S13).

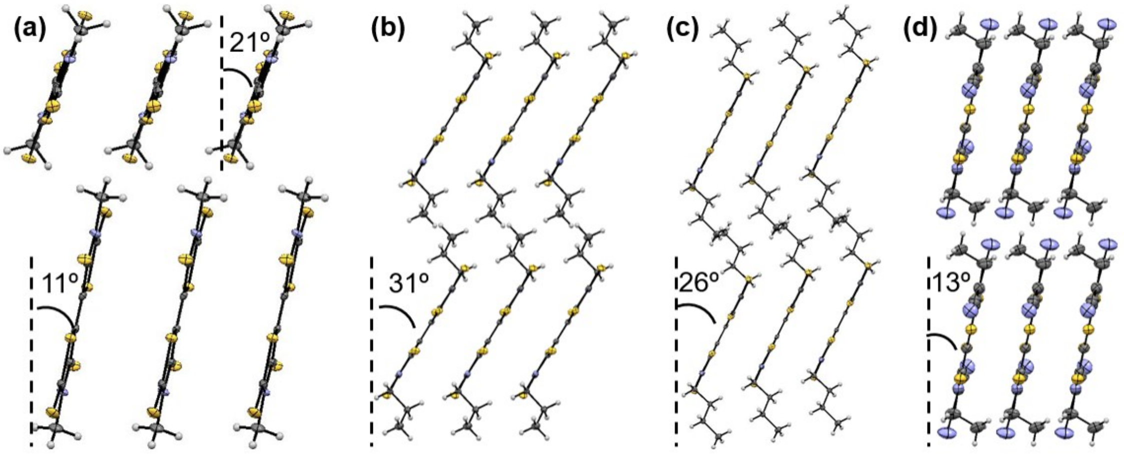

Figure S12. Tilt angles of (a) **SS-Me**, (b) **SS-Pr**, (c) **SS-Bu**, and (d) **S(CN)$_2$-Bu**.

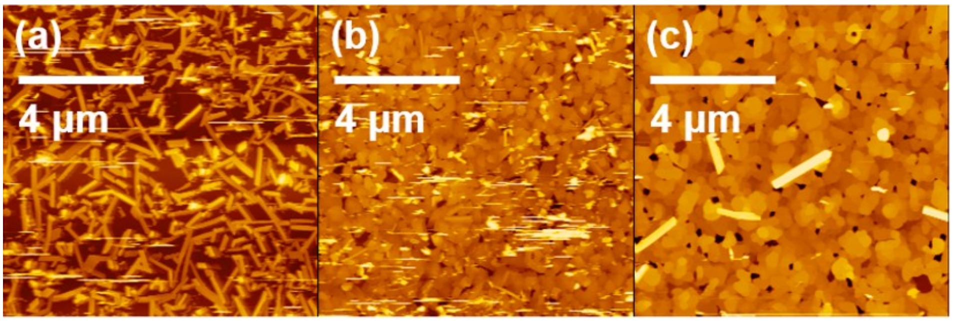

Figure S13. AFM images of (a) **SS-Me**, (b) **S(CN)$_2$-Et**, and (c) **SO-Et**.

References

S1 K.-J. Baeg, Y.-Y. Noh, J. Ghim, B. Lim and D.-Y. Kim, *Adv. Funct. Mater.*, 2008, **18**, 3678.

S2 K. Shibata, H. Wada, K. Ishikawa, H. Takezoe, T. Mori, *Appl. Phys. Lett.*, 2007, **90**, 193509.

S3 M. C. Burla, R. Caliandro, M. Camalli, B. Carrozzini, G. L. Cascarano, L. De Caro, C. Giacovazzo, G. Polidori, D. Siliqi and R. Spagna, *J. Appl. Crystallogr.*, 2007, **40**, 609–613.

S4 G. M. Sheldrick, *Acta Crystallogr. Sect. A Found. Crystallogr.*, 2007, **64**, 112–122.

S5 T. Mori, A. Kobayashi, Y. Sasaki, H. Kobayashi, G. Saito and H. Inokuchi, *Bull. Chem. Soc. Jpn.*, 1984, **57**, 627–633.